

COMPUTATIONAL METHOD FOR A GRADIENT-ENHANCED DAMAGE THEORY

Stella Pires Domingues^a, Heraldo Costa Mattos^a and Fernando Alves Rochinha^b

^a *Department of Mechanical Engineering, Universidade Federal Fluminense, Stella@vm.uff.br,
<http://www.uff.br>*

^b *Department of Mechanical Engineering, POLI/COPPE, Universidade Federal do Rio de Janeiro,
<http://www.ufrj.br>*

Keywords: Damage Mechanics; Finite Elements; Splitting Technique.

Abstract: In the last years different continuum damage theories have been proposed to describe the behavior of elastic materials. Among these theories, some introduce higher order gradients of the damage variable in the constitutive model, in order to avoid the loss of well-posedness in the post-localization range. Although such theories allow a mathematically correct modelling of the strain localization phenomena, they are usually considered complex to handle from the numerical point of view. The present work is concerned with the numerical implementation of a gradient-enhanced damage theory for elastic materials. A simple numerical technique, based on the finite element method, is proposed to approximate the solution of the resulting nonlinear mathematical problem. The coupling between damage and strain variables is circumvented by means of a splitting technique, which permit to transform the nonlinear coupled problem in a sequence of simpler linear problems. In order to evaluate the physical coherence of the model and to access the main features of the numerical method some problems and different numerical techniques are analyzed.

1 INTRODUCTION

In the last few years, many different continuum damage theories have been proposed. Since the damage propagation generally leads to a local softening behaviour, the models based on a local approach, see [Kachanov \(1986\)](#) and [Lemaitre and Chaboche \(1990\)](#), may lead to a physically unrealistic description of strain localization phenomena when the hypothesis of quasi-static and isothermal processes are considered. In general, due to the loss of ellipticity of the governing equations in the post-localization range, the resulting mathematical problems may present an infinity number of solutions with discontinuous fields of displacement gradients what leads to numerical difficulties of mesh-dependence, see [Knowles and Sternberg \(1978\)](#); [Pietruszczak and Mróz \(1981\)](#); [Needleman \(1987\)](#); [Bazant and Cabot \(1988\)](#); [Vree et al \(1995\)](#).

Some alternative approaches to the local damage theories have been proposed in the last years, see [Saouridis and Mazars \(1988\)](#); [Bazant and Cedolin \(1991\)](#); [Costa-Mattos et al \(1992\)](#); [Frémond and Nedjar \(1996\)](#), for example. The present paper deals with an alternative theory in which the continuum is supposed to possess a microstructure. Since damage results from microscopic movements, it is proposed a reformation of the kinematics and of some basic governing principles of the classical Continuum Mechanics in order to account for such “micromovements”. The constitutive equations are developed within a thermodynamic framework - the free energy is supposed to depend not only on the strain and the damage variable but on the damage gradient as well. Besides, to account for microscopic effects, the power of the internal forces depends not only on the velocity and its gradient, but also on the damage velocity and its gradient

The contribution is complete the presentation of a numerical technique for approximating the resulting nonlinear mathematical problems [Pires-Domingues et al \(1999\)](#). The coupling between damage and strain is circumvented by means of a splitting technique which allows study the nonlinear problem through a sequence of simpler linear problems. This technique requires, at each time step, the solution of two problems: one similar to an equilibrium problem in linear elasticity and the other similar to a heat transfer problem in a rigid body. In order to assess the main features of the numerical method, a number of examples are presented showing that the numerical computations are not mesh dependent.

2 MODELLING

A body is defined as a set of material points B which occupies a region Ω of the Euclidean space at the reference configuration. In this theory, besides the classical variables that characterize the kinematics of a continuum medium (displacements and velocities of material points), an additional scalar variable $\beta \in [0,1]$, is introduced. This variable is related with the links between material points and can be interpreted as a measure of the local cohesion state of the material. If $\beta = 1$, all the links are preserved and the initial material properties are preserved. If $\beta = 0$, a local rupture is considered since all the links between material points have been broken. The variable β is associated to the damage variable D by the following relation: $\beta = 1 - D$. Since the degradation is an irreversible phenomenon, the rate $\dot{\beta}$ must be negative or equal to zero.

A detailed presentation of the basic principles that govern the evolution of such kind of continuum can be found in [Costa-Mattos and Sampaio \(1995\)](#); [Pires-Domingues \(1996\)](#). A summary of the basic principles are presented in this section. For the sake of simplicity the hypothesis of quasi-static and isothermal processes is adopted throughout this work. Besides

it is also assumed the hypothesis of small deformation and consequently the conservation of mass principle is automatically satisfied.

2.1 The principle of virtual power

Let a body B that occupies a region $\Omega \subset \mathbb{R}^3$ with a sufficiently regular boundary Γ be subjected at each time instant t to external forces $g(t) : \Gamma_2 \subset \Gamma \rightarrow \mathbb{R}^3$, $b(t) : \Omega \rightarrow \mathbb{R}^3$ to external microscopic forces $p(t) : \Omega \rightarrow \mathbb{R}$, $q(t) : \Gamma_2 \subset \Gamma \rightarrow \mathbb{R}$ and to prescribed displacements $u(t) = 0$ em $\Gamma_1 \subset \Gamma$, where $\Gamma = \Gamma_1 \cup \Gamma_2$ and $\Gamma_1 \cap \Gamma_2 = \emptyset$.

Under the hypothesis of slow deformations, the inertial effects can be neglected and the principle of Virtual Power can be expressed as:

$$\pi_{\text{int}} + \pi_{\text{ext}} = 0 \quad (1)$$

for any admissible variations of the fields (u and β) that characterize the kinematics of the medium.

The power π_{int} of the internal generalized forces σ , F and H can be written as:

$$\pi_{\text{int}} = -\int_{\Omega} (\sigma \cdot \nabla \hat{u}) dV - \int_{\Omega} (F \hat{\beta} + H \cdot \nabla \hat{\beta}) dV \quad (2)$$

Here $\hat{u} : \Omega \rightarrow \mathbb{R}^3$ is an element of the set V_v of the virtual velocities \hat{u} such that $\hat{u}|_{\Gamma_1} = 0$ and $\hat{\beta} : \Omega \rightarrow \mathbb{R}$ is an element of the set V_{β} of the virtual variations of β .

The corresponding power π_{ext} of the external generalized forces b , g , p and q assumes the representation:

$$\pi_{\text{ext}} = \int_{\Omega} (b \cdot \hat{u}) dV + \int_{\Gamma_2} (g \cdot \hat{u}) dA + \int_{\Omega} (p \hat{\beta}) dV + \int_{\Gamma} (q \hat{\beta}) dA \quad (3)$$

Where $p : \Omega \rightarrow \mathbb{R}$ is defined as a microscopic distance force while $q : \Gamma \rightarrow \mathbb{R}$ is a microscopic contact force, both in duality with β . The microscopic forces are related to non mechanical actions (chemical and electromagnetic, for instance), that can cause an evolution of the damage.

Under assumptions of π_{int} and π_{ext} and the hypothesis of slow deformations, the inertial effects can be neglected and the principle of virtual power can be expressed as:

$$\int_{\Omega} [\sigma \cdot (\nabla \hat{u}) - b \cdot \hat{u}] dV - \int_{\Gamma_2} (g \cdot \hat{u}) dA + \int_{\Omega} [H \cdot (\nabla \hat{\beta}) + F \hat{\beta} - p \hat{\beta}] dV - \int_{\Gamma} (q \hat{\beta}) dA = 0, \quad \forall \hat{u} \in V_v, \quad \forall \hat{\beta} \in V_{\beta} \quad (4)$$

2.2 Constitutive equations

Under the hypothesis of small deformations and isothermal processes, the free energy is supposed to be a function of the deformation ϵ , the temperature θ , the damage variable β and its gradient $\nabla \beta$. In order to resume the presentation, the thermodynamic framework used to obtain the constitutive equations is not presented in this paper, for further details see [Costa-Matts and Sampaio \(1995\)](#). The final relations are the following:

$$\sigma = \left(\frac{\beta E}{1 + \nu} \right) \left[\frac{\nu}{1 - 2\nu} \text{tr}(\epsilon) \mathbf{I} + \epsilon \right] = \beta [\lambda (\text{tr} \epsilon) \mathbf{I} + 2\mu \epsilon] \quad (5)$$

$$F = \left(\frac{E}{2(1+\nu)}\right) \left[\frac{\nu}{(1-2\nu)} (\text{tr}(\boldsymbol{\varepsilon}))^2 + \boldsymbol{\varepsilon} : \boldsymbol{\varepsilon} \right] - w + \lambda_{\beta} + C\dot{\beta} + \lambda_{\dot{\beta}} =$$

$$= \left[\frac{1}{2} \lambda (\text{tr} \boldsymbol{\varepsilon})^2 + \mu \boldsymbol{\varepsilon} : \boldsymbol{\varepsilon} \right] - w + \lambda_{\beta} + C\dot{\beta} + \lambda_{\dot{\beta}} \quad (6)$$

$$H = k(\nabla\beta) \quad (7)$$

Where E is the Young modulus, ν is the Poisson's ratio and λ and μ are the Lamé constants. The terms λ_{β} and $\lambda_{\dot{\beta}}$ are lagrange multipliers associated, respectively, to the constraints $\beta \geq 0$ and $\dot{\beta} \leq 0$, they are such that: $\lambda_{\beta} \leq 0$, $\beta \lambda_{\beta} = 0$ and $\lambda_{\dot{\beta}} \leq 0$, $\dot{\beta} \lambda_{\dot{\beta}} = 0$.

2.3 The model parameters

The proposed model has different parameters to simulate the Damage evolution in different brittle materials. The most important model parameters are k , C and w . They can be estimated from a non-homogeneous one-dimensional model, [Pires-Domingues \(1996\)](#). Another proceeding is chose a standard test and adapt the numerical and experimental curves. The C coefficient is related to the material viscosity; k is related to damage localization; w is the elastic deformation energy.

The non-homogeneous one-dimensional model was used to simulate the behaviour of a specimen loaded by a prescribed displacement, $u(t)$, with the following characteristics: E (Young modulus or modulus of elasticity) equal 50.0GPa, w (elastic deformation energy) equal 0.025MPa, L (length) equal 1.0m and α (loading velocity) equal 5.0×10^{-3} m/s. The figures 1 and 2 present the results for different k (and $C = 0.1\text{MPa}\cdot\text{s}$) and C (and $k = 0.1\text{MPa}\cdot\text{m}^2$) parameters.

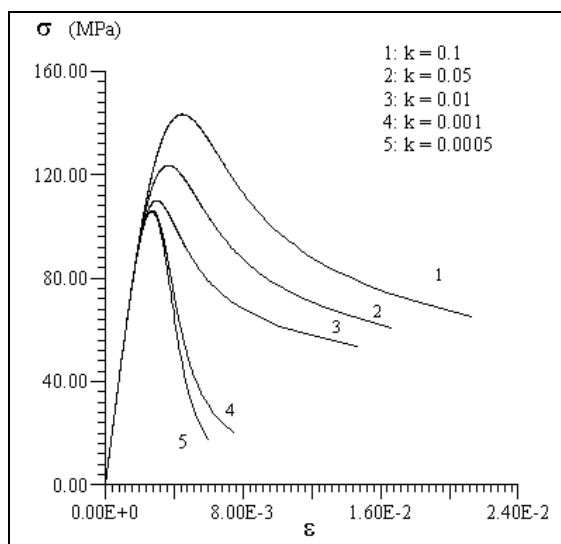


Figure 1: $\sigma \times \varepsilon$ with different k

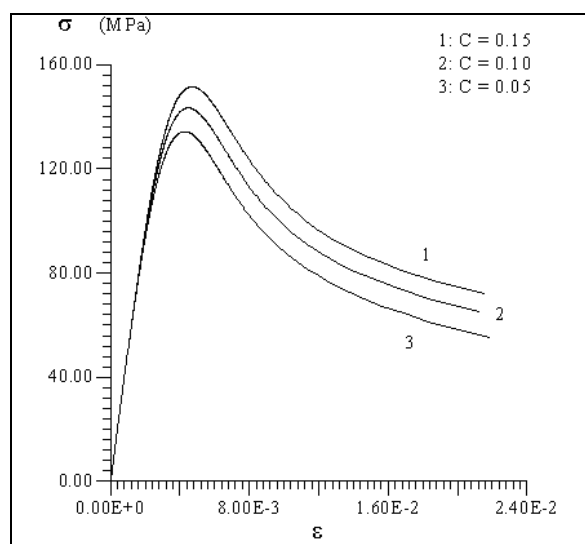


Figure 2: $\sigma \times \varepsilon$ with different C

It can be observed that small value of k result in damage more localized in the material, figure 1, and the material broke more quickly for C small, figure 2.

More details about the non-homogeneous one-dimensional model can be found in [Pires-Domingues \(1996\)](#).

3 THE MECHANICAL PROBLEM

Introducing the constitutive equations (5), (6) in (4), neglecting the external microscopic forces (which are related to chemical or electromagnetic actions) and considering the initial conditions: $\beta(x, t = 0) = 1, \forall x \in \Omega$, the following mathematical problem is obtained:

Find $(u(x, t), \beta(x, t))$, respectively the displacement field $u(t) : \Omega \rightarrow \mathbb{R}^3$ such that $u(t)|_{\Gamma_1} = \bar{u}(t)$ and the field $\beta(t) : \Omega \rightarrow \mathbb{R}$ such that, for all time instant $t \in [0, \tau]$:

$$\int_{\Omega} \beta(t) [\lambda \operatorname{div} u \operatorname{div} \hat{u} + 2\mu \boldsymbol{\varepsilon}(u) \cdot \boldsymbol{\varepsilon}(\hat{u})] dV - \int_{\Omega} b(t) \cdot \hat{u} dV - \int_{\Gamma_2} g \cdot \hat{u} dA = 0 \quad \forall \hat{u} \in V_v \quad (8)$$

$$\int_{\Omega} (k \nabla \beta) \cdot \nabla \hat{\beta} dV + \int_{\Omega} \left[\frac{1}{2} \lambda (\operatorname{div} u)^2 + \mu \boldsymbol{\varepsilon} \cdot \boldsymbol{\varepsilon} - w \right] \hat{\beta} dV + \int_{\Omega} C \hat{\beta} dV = 0 \quad \forall \hat{\beta} \in V_{\beta} \quad (9)$$

Subjected to the following constraints:

$$0 \leq \beta \leq 1 \quad \text{e} \quad \dot{\beta} \leq 0$$

And with the following initial condition:

$$\beta(t = 0) \equiv 1$$

4 NUMERICAL APROXIMATION

The nonlinear mathematic damage evolution problem resulting from the model, accounting for the coupling between damage and displacement fields, can be solved through a staggered algorithm, in which the coupled system is partitioned, often according to the different coupled fields, and each partition can be treated by a different time-stepping algorithm.

The approach proposed in this work is motivated by the realization that a partition of the coupled system only defines an operator split of the evolution problem. In this context, a staggered scheme is viewed as a product formula algorithm dictated by the specific operator split, exactly as in the classical method of fractional steps, see [Yanenko \(1980\)](#). This point of view is also adopted in [Simo and Miehe \(1992\)](#), where standard staggered algorithms for coupled thermo-mechanical problems, consisting of an isothermal phase followed by a heat conduction phase at fixed configuration, are cast into the format of a fractional step method.

4.1 Semi-discrete problem: finite element method

The solution of the damage evolution problem is based on a spatial discretization using the Finite Element Methods (FEM) leading in a semi-discrete version constituted of a nonlinear system of Ordinary Differential Equations (EDO). This system is accomplished by means of a splitting strategy resulting in a sequence of simpler evolution problems, which are in turn solved by standard techniques like backward and forward Euler and the trapezoidal rule, see [Hughes \(1987\)](#).

Let the base function (or interpolation function) traditionally provided by the MEF, see [Hughes \(1987\)](#), $N_i \in V_v^h$, where V_v^h is a finite sub-space of the space V_v , and $\varphi_i \in V_{\beta}^h$, where V_{β}^h is a finite sub-space of the space V_{β} . These base functions allow the construction of the following approximations:

$$u_h(x, t) = \sum_{i=1}^{m_h} u_i(t) N_i(x), \quad i = 1, \dots, m_h$$

$$\beta_h(x, t) = \sum_{i=1}^{m_h} \beta_i(t) \varphi_i(x), \quad i = 1, \dots, m_h \quad (10)$$

Where m_h is the nodal point number of the finite element mesh and h is the mesh parameter, a scalar that is associated with the mesh refinement.

The semi-discrete problem is obtained by replacing u by u_h and β by β_h , defined by equation (10), in equations (8) and (9). The semi-discrete problem is a nonlinear system of ordinary differential equations with the following form:

$$\mathbf{K}[\beta_h] \underline{u} = \mathbf{R} \quad (11)$$

$$\mathbf{C} \dot{\underline{\beta}} + \mathbf{A} \underline{\beta} + \mathbf{F}(\underline{u}) = 0 \quad (12)$$

With the following initial condition:

$$\beta_h(x, 0) = 1 \quad e \quad u_h(x, 0) = 0$$

And the following constraints:

$$0 \leq \beta_h(x, t) \leq 1 \quad e \quad \dot{\beta}_h(x, t) \leq 0.$$

Where,

$$[\mathbf{K}(\beta_h)]_{ij} = \int_{\Omega} \beta_h [\mathbf{B}^T \mathbf{D} \mathbf{B}]_{ij} dV, \quad i, j = 1, \dots, 3 * m_h \quad (13)$$

$$[\mathbf{R}]_i = \int_{\Omega} b_k N_i dV - \int_{\Gamma} g_k N_i dA ; \quad (14)$$

$$[\mathbf{C}]_{ij} = \int_{\Omega} C \varphi_i \varphi_j dV, \quad i, j = 1, \dots, m_h \quad (15)$$

$$[\mathbf{A}]_{ij} = \int_{\Omega} (k \nabla \varphi_i \nabla \varphi_j) dV, \quad i, j = 1, \dots, m_h ; \quad (16)$$

$$[\mathbf{F}(\underline{u})]_i = \int_{\Omega} \left[\frac{1}{2} (\overline{\mathbf{B}^T \mathbf{D} \mathbf{B}} \underline{u} \cdot \underline{u}) - w \right] \varphi_i dV, \quad i, j = 1, \dots, m_h \quad (17)$$

\mathbf{B} denotes the standard discretized differential operator and \mathbf{D} is the matrix of the elastic constitutive coefficients, defined according Hughes (1987).

4.2 Operator split technique applied to the semi-discrete problem

The Operator Split Technique is used to approximate the nonlinear semi-discrete problem through a sequence of simpler linear problems. Two partitions of operator were considered, one related to u_h (“equilibrium problem”) and the other to β_h (“damage evolution problem”). The proposed scheme can result in two different algorithms depending on the order of the sequence of the operators. These algorithms, resumed below, will be named DANO_1 and DANO_2.

The DANO_1 algorithm first solves the “damage evolution problem”, remaining the displacement field unaltered. At this first stage, the associated ordinary differential equation is solved using a time integration method, that can be described as:

$$\begin{aligned} & \mathbf{C} [\theta \beta^{n+1} + (1 - \theta) \hat{\beta}^n] + \Delta t [\theta \mathbf{A} \beta^{n+1} + (1 - \theta) \mathbf{A} \beta^n] + \\ & + \Delta t^n [\theta \tilde{\mathbf{F}}^{n+1} + (1 - \theta) \mathbf{F}^n] = 0 \end{aligned} \quad (18)$$

Where, θ define the integration method: $\theta = 0$, forward Euler; $\theta = 1$, backward Euler and $\theta = 1/2$, trapezoidal rule, see [Hughes \(1987\)](#). The subscript h was omitted and the superscript n means that the function is approximated at the instant t_n . Besides, \tilde{F}^{n+1} does not represent the function F evaluated at t_{n+1} , since u_{n+1} is not known. At the first phase ($\dot{u} = 0$) \tilde{F}^{n+1} is calculated using u_n .

The second phase of DANO_1 solves the "equilibrium problem":

$$\mathbf{K}(\beta_{n+1}) \underline{u}_{n+1} = \mathbf{R}_{n+1} \quad (19)$$

Where,

$$[\mathbf{R}_{n+1}]_i = \int_{\Omega} (b_k)_{n+1} N_i dV - \int_{\Gamma} (g_k)_{n+1} N_i dA \quad (20)$$

The DANO_2 algorithm consists in the order inversion of the stages of DANO_1. The computational implementation of the two algorithms can be considered simple, since both algorithms can be obtained from a standard finite element scheme. It can be observed that "damage evolution problem" phase is similar to a heat conduction problem, while the other phase, the "equilibrium problem", is similar to a classical elasticity problem.

5 ANALYSIS OF NUMERICAL EXAMPLES

In order to assess the features of the modelling in a three-dimensional stress state, problems of a double edge cracked plate and of a square plate with a central circular hole is analyzed, [Domingues \(1999\)](#).

The square plate (200 mm x 200 mm x 1 mm) with a central circular hole, which radius is 50 mm, is supported at the left side and loaded with a prescribed displacement $u(t)$ at the opposite side, figure 3. Due to symmetry of the problem the analysis is performed for the upper right quarter of the plate only.

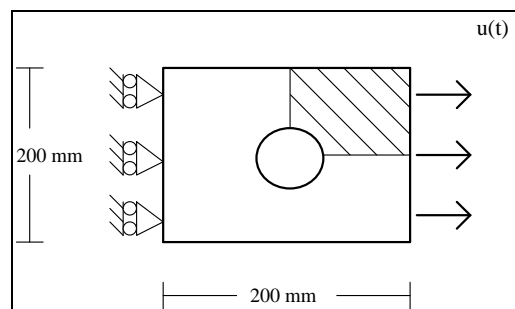


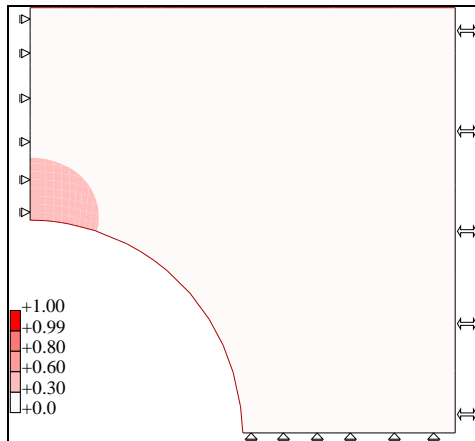
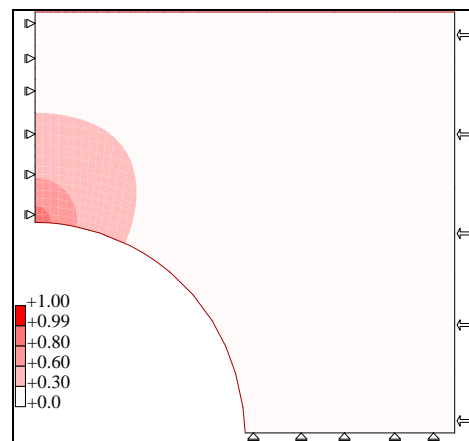
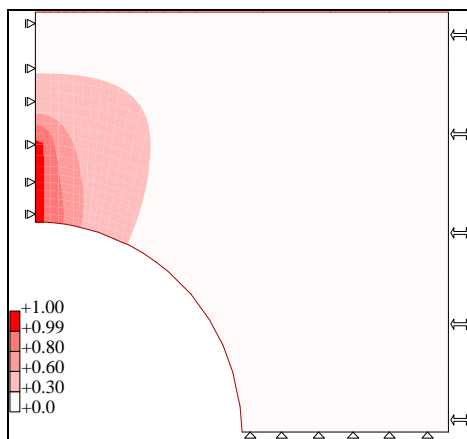
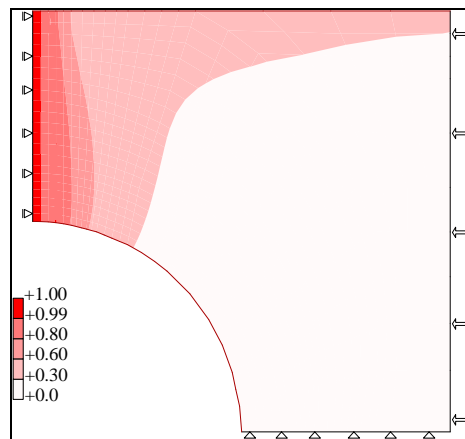
Figure 3: Plate with a central circular hole.

In this study was considered a plate of concrete, which has the following mechanical characteristics: $E = 27.0$ GPa, $w = 5.0 \times 10^{-5}$ MPa, $C = 1.0 \times 10^{-3}$ MPa.s and $k = 0.2$ MPa.mm², see [Frémond and Nedjar \(1996\)](#). The prescribed displacement and the adopted time step are respectively given by $u(L, t) = \alpha t$, ($\alpha = 5.0 \times 10^{-3}$ mm/s) and $\Delta t = 1.0 \times 10^{-4}$ s, respectively. The usual bi-linear quadrilateral finite element is used. Other examples are presented in [Pires-Domingues \(2004\)](#).

5.1 Damage propagation

The evolution of the damage variable $D = (1 - \beta)$ on the plate is depicted in figures 4 up to 7. These figures demonstrate that the damage initially appear at a local near the hole, see

figures 4 and 5, what is expected for a body with this kind of geometry and submitted to a tension load. Then the damage propagates in the direction of the free end of the plate, perpendicular to the load direction, until the plate is broken completely.

Figure 4: Damage levels, $t = 2.5$ s.Figure 5: Damage levels, $t = 2.8$ s.Figure 6: Damage levels, $t = 3.0$ s.Figure 7: Damage levels, $t = 3.35$ s.

The figure 8 presents a curve of the external force versus the displacement $u(t)$ prescribed at the extremity, which represents the global behaviour of the structure, allowing to observe the softening behaviour.

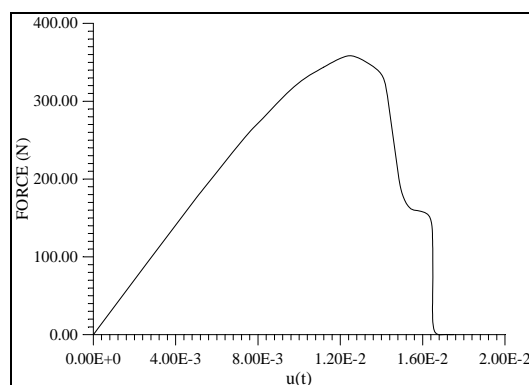


Figure 8: Force versus displacement.

5.2 Mesh dependence

To show that the problem solution is not mesh-dependent four different spatial discretization meshes were used. The meshes are presented in the figures 9 up to 12. The difference between these meshes is the degree of the discretization in the region where the highest levels of damage occur. In spite of the mesh-1 and mesh-4 (figures 9 and 12, respectively) have 274 nodes and 240 elements, the difference between these meshes are the distortion region in the last one.

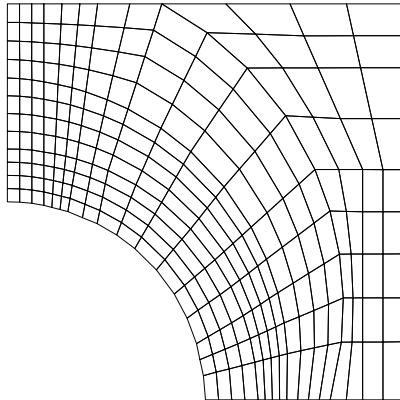


Figure 9: Mesh-1 (274 nodes and 240 elem.).

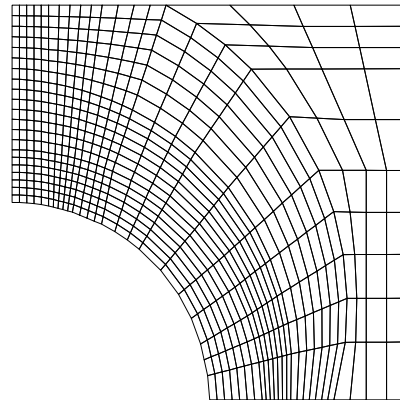


Figure 10: Mesh-2 (594 nodes and 544 elem.).

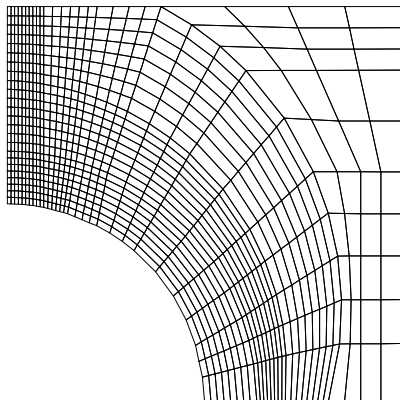


Figure 11: Mesh-3 (819 nodes and 760 elem.).

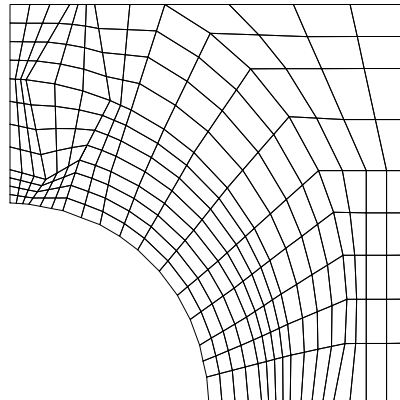


Figure 12: Mesh-4 (274 nodes and 240 elem.).

The figures 14 and 15 permit to observe the damage propagation along the horizontal lines A ($y = 53.0$ mm) and B ($y = 60.0$ mm), figures 16. The shapes of the curves and the damage levels at different points along those lines are almost the same for different meshes. The same behaviour is observed for stress and displacement fields, see [Carmeliet and Borst \(1995\)](#).

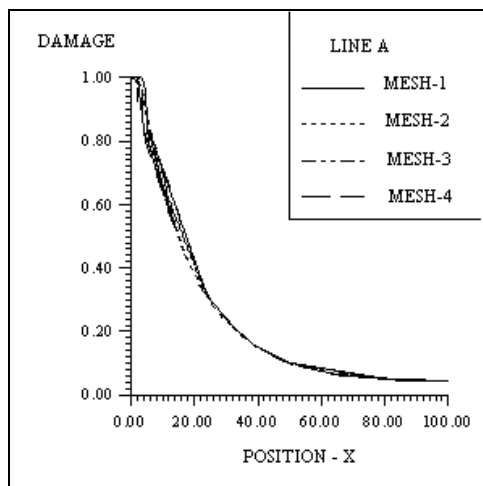


Figure 14: Damage along the lines A.

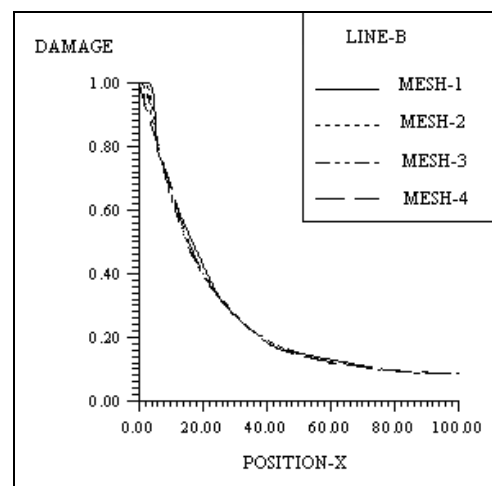


Figure 15: Damage along the lines B.

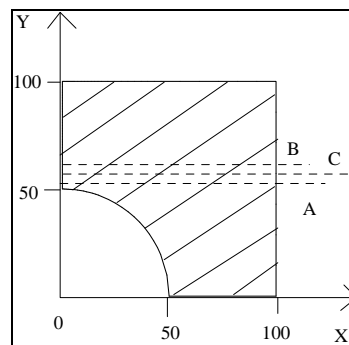


Figure 16: Longitudinal lines A, B and C.

The curves of the applied forces versus displacement obtained using the different meshes are presented in the figure 17 to complete the mesh dependence analysis. The results represent the behaviour of the global structure. The different mesh discretizations not affect the results. Figure 16 also permit to observe the softening behaviour.

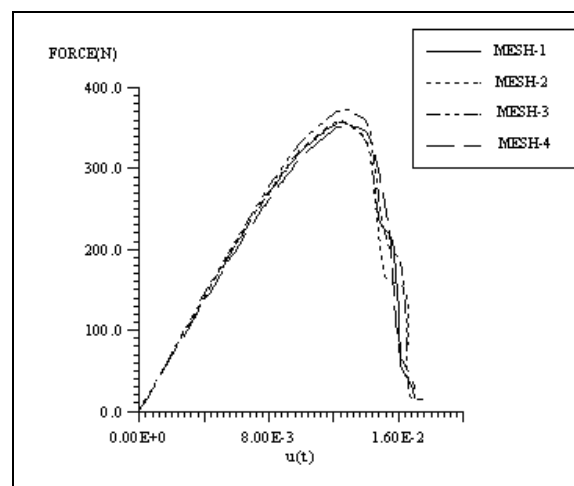


Figure 17: Force versus displacement for different meshes.

In order to complete the mesh-dependence analysis the problem of a double edge cracked plate is exploited. The double edge cracked plate contains crack length $a = 4$ mm, length $L =$

25 mm and width $W = 10$ mm, is loaded with a prescribed displacement $u(t)$ at the both sides, figure 18.

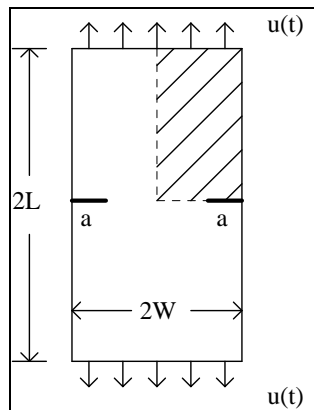


Figure 18: Double edge cracked plate.

The existent symmetry permits to analyze only a quarter of the plate, in that case the upper right quarter of the plate, see figure 18.

In this study was considered plates of concrete, which have the following mechanical characteristics: $E = 27.0$ GPa, $w = 5.0 \times 10^{-5}$ MPa, $C = 1.0 \times 10^{-3}$ MPa.s and $k = 0.2$ MPa.mm², see Frémond (1996) and Pires-Domingues (1996). The prescribed displacement and the adopted time step are given respectively by $u(L,t) = \alpha t$, ($\alpha = 5.0 \times 10^{-3}$ mm/s) and $\Delta t = 1.0 \times 10^{-4}$ s.

The usual bi-linear quadrilateral finite element is used on the discretization of the problem. The different meshes employed on the evaluation of the problem are depicted on the figure 19. The mesh-1 has 340 nodes and 304 elements, the mesh-2 has 500 nodes and 456 elements and the mesh-5 has 252 nodes and 221 elements. The mean difference among the meshes is the degree of the discretization and the distorted in the region where the highest levels of damage are expected.

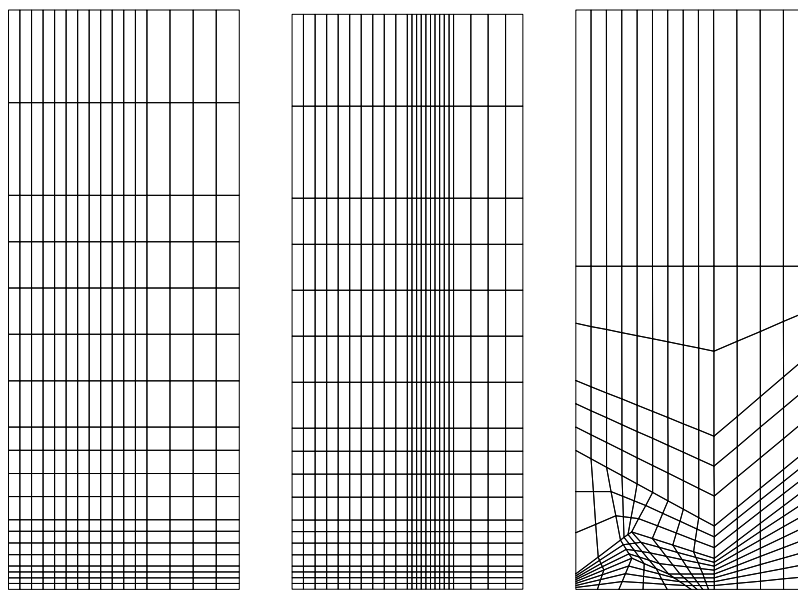


Figure 19: Mesh-1

Mesh-2

Mesh-3

The figure 20 shows the instants of maximum damage for the 3 different meshes. The damage levels obtained using different meshes are practically the same, meaning that the problem solution is not mesh-dependent. Due the degree of spatial discretization in the region where the highest levels of stress and damage are expected, the instants of maximum damage are slightly different for each mesh. The moment of complete degradation of the material (plate completely broken into two parts that experiment rigid body movement) can be also determined observing the stress and displacement levels on the plate, see Pires-Domingues (1996).

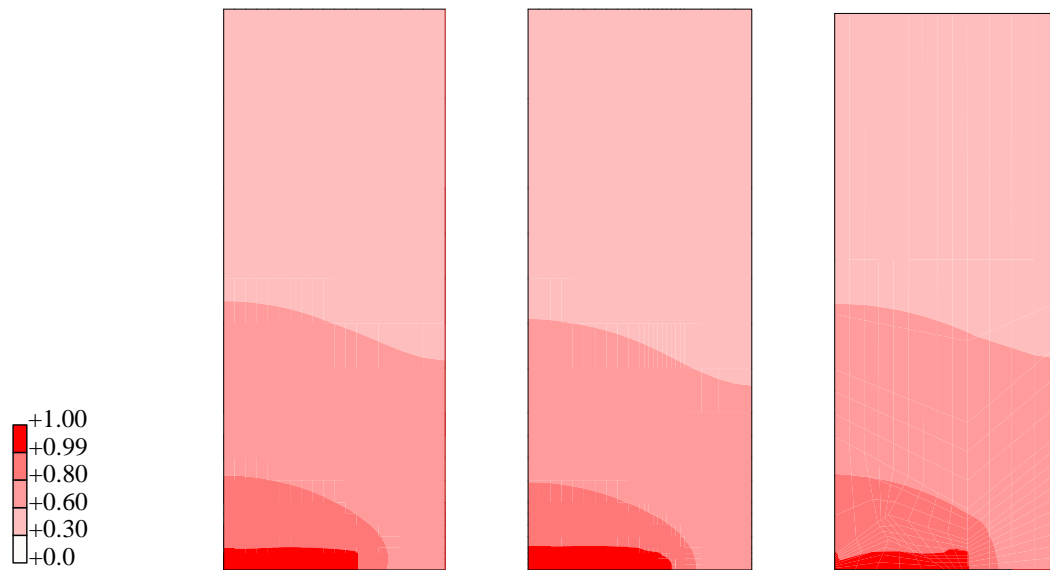


Figure 20: Mesh-1 (t=1.585s) Mesh-2 (t=1.577s) Mesh-3 (t=1.59s)

In order to complete the mesh-dependence analysis the curves of the external force versus the displacement $u(t)$, obtained employing the 3 different meshes, are presented in the figure 21. These curves represent the global behaviour of the structure. It is possible to observe that the shape of the solution is not affected by the different spatial discretization in the region where highest levels of stress are expected. The reason of the slight difference of applied force values (on the top of the curves) is due a better discretization in critical region of mesh-2, that permit a better approach of the equations. The curves also permit to observe the expected softening behaviour.

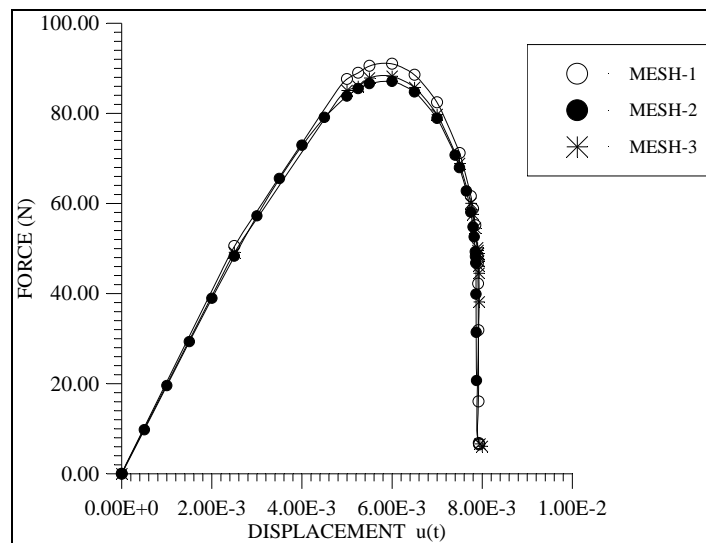


Figure 21: External force x Prescribed displacement.

5.3 Stability and precision of the proposed algorithm

The performance of the proposed algorithm is examined by comparison the results of the variable β and u obtained from different time increments Δt and using the same spatial discretization, mesh-2, figure 10. The DANO_1 algorithm and the integration method, backward Euler ($\theta = 1$) were employed.

The time increments observed were 0.1 s, 0.01 s, 0.001 s, 0.0005s e 0.0001 s. The β and u_y results for points on the line B, at $t = 3.0s$, are presented in the figures 22 and 23. The time increments 0.0005 and 0.0001s present the same values in different points along line B.

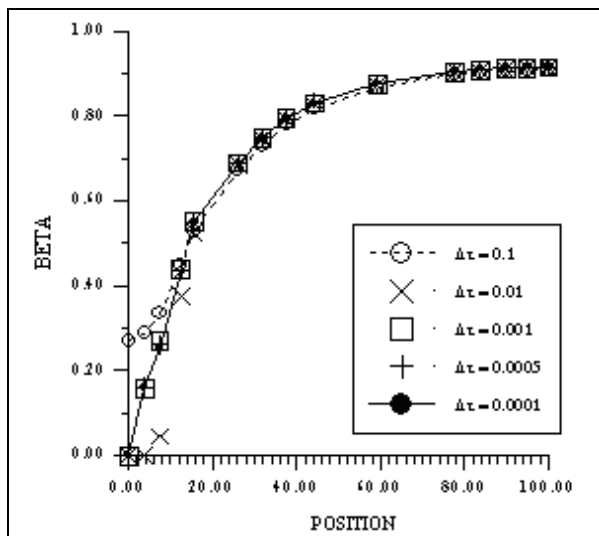


Figure 22: β values at $t = 3.0s$.

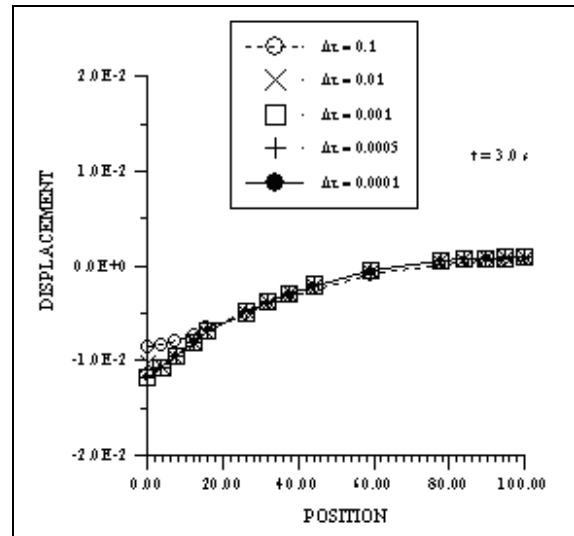


Figure 23: u_y values at $t = 3.0s$.

The precision analysis of the proposed algorithm consists of comparing the results obtained using the operator split methods with different numerical integration methods (forward and backward Euler and trapezoidal rule) and the results of a coupled solution strategy, where the Euler and Newton Methods are used together to solve the non-linear resultant system. The β and displacement results, at $t = 3.2s$, are shown in figures 24 and 25. The analysis employed

Mesh-1, figure 9, for both strategy and $\Delta t = 0.0001s$ for the operator split methods (DANO_1) and $\Delta t = 0.00001s$ for the coupled solution strategy. The points of the longitudinal line C ($y = 56.0mm$) were observed in this analysis. The different symbols represent the following: (O) backward Euler; (●) forward Euler; (□) trapezoidal rule and (*) coupled solution.

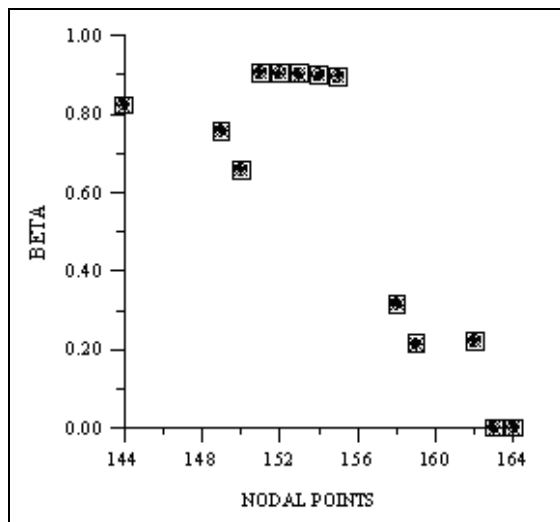


Figure 24: β values, $t = 3.2s$.

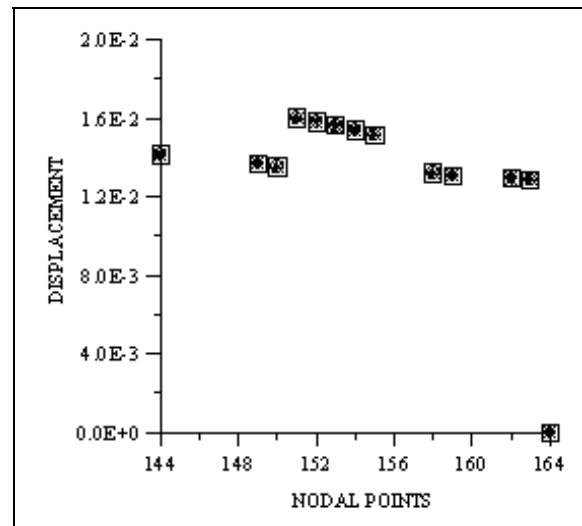


Figure 25: Displacement values, $t = 3.2s$.

It can be observed that the results are similar employing different algorithms. The results presented prove that the operator split method was able to give the results at the same precision level that other methods capable of solving the coupled problem. The last method is more expensive because the computational time to solve the problem.

6 CONCLUSIONS

The gradient-enhanced damage theory presented in this paper can describe the non-linear evolution of the damage, the stress and the displacement fields on a plate formed by elastic brittle materials (concrete, glass and ceramic, for instance). Besides, it allows a mathematically correct description of the localization and the strain-softening phenomena without problems of mesh dependence [Pires-Domingues \(1996\)](#).

Despite the strong nonlinearity of the constitutive equations, a simple numerical technique, resulting from the combination of the finite element discretization and a operator split technique [Pires-Domingues \(1996\)](#), is used in other to approximate the solution of the mathematical problem. Such numerical strategy allows handle the nonlinear global problem through a sequence of linear problems. Hence, this solution technique can be easily implemented from a standard finite element code for linear problems without the necessity of radical modifications. It is also important to emphasize that the algorithm has shown in the numerical examples has good stability and precision, and has demonstrated no evidence of mesh dependence. The numerical method also allows a correct mathematical description of the localization phenomena and the softening behaviour without present mesh-dependence [Carmeliet and Borst \(1995\)](#). More information about the model and the numerical method can be found in [Pires-Domingues \(1996\)](#).

REFERENCES

- Bazant, Z.P., and Cedolin, L., "Stability of Structures - Elastic, Inelastic and Damage Theories", *Oxford University Press* (1991).
- Bazant, Z.P., and Pijandier Cabot, G., "Nonlocal Continuum Damage, Localisation, Instability and Convergence", *ASME J. Appl. Mech.*, Vol. 55, pp. 287-293 (1988).
- Carmeliet, J., and Borst, R. de, "Stochartic Approaches for Damage Evolution in Standard and N Continua", *Int. J. for Solids and Structures*, Vol. 32, N°8/9, pp. 1160 (1995).
- Costa-Mattos, H., and Sampaio, R., "Analysis of the Fracture of Brittle Elastic Materials Using a Continuum Damage Model", *Structural Engineering and Mechanics*, Vol. 3, N°5, pp. 411-428 (1995).
- Costa-Mattos, H., Frémond, M., and Mamiya, E.N., "A Simple Model of the Mechanical Behavior of Ceramic-Like Material", *Int. J. for Solids and Structures*, Vol. 20, N° 24, pp. 3185-3200 (1992).
- Domingues, S.M.P., Costa-Mattos, H., and Rochinha, F.A., "Evolução Não-linear de Dano em Materiais Elásticos e Frágeis: Modelagem e Simulação Numérica", *Revista Internacional de Métodos Numéricos para Cálculo y Diseño en Ingeniería*, Vol. 15. 3, 315-327 (1999).
- Frémond, M., and Nedjar, B., "Damage, Gradient of Damage and Principle of Virtual Power", *Int. J. Solids Structures*, Vol. 33, N° 8, pp. 1083-1103 (1996).
- Hughes, T.J., "The Finite Element Method, Linear Static and Dynamic Finite Element Analysis", *Prentice-Hall* (1987).
- Kachanov, L.M., "Introduction to Continuum Damage Mechanics", *Martinus Nijhoff Publishers, Dordrecht, Netherland* (1986).
- Knowles, J.K., and Sternberg, E., "On the Failure of Ellipticity and the Emergence of Discontinuous deformation Gradients in Plane Finite Elastostatics", *J. Elasticity*, 8, 329-378 (1978).
- Lemaitre, J. and Chaboche, J.L., "Mechanics of Solid Materials", *Cambridge University Press* (1990).
- Needleman, A., "Material Rate Dependence and Mesh Sensitivity in Localisation Problems", *Comput. Meths. Appl. Mech. Engineering*, Vol. 67, pp. 69-87 (1987).
- Pietruszczak, S.T., and Z. Mróz, "Finite Element Analysis of Deformation of Strain-Softening Materials", *Int. J. Numer. Methods Eng.*, Vol. 17, pp. 327-334 (1981).
- Pires-Domingues, S.M., "Análise de Materiais Elásticos Frágeis através de um Modelo de Dano Contínuo", *Doctoral Thesis*, Pontifícia Universidade Católica do Rio de Janeiro - PUC-Rio (1996).
- Pires-Domingues, S.M., Costa-Mattos, E., and Rochinha, F.A., "Nonlinear Elastic Brittle Damage: Numerical Solution by Means of Operator Split Methods", *Journal of Theoretical and Applied Mechanics*, 4, 37, 1999.
- Pires-Domingues, S.M., Costa-Mattos, H., and Rochinha, F.A., "Modeling of Macro-Crack Initiation and Propagation in Elastic Structures using a Continuum Damage Model", *2ndSAE Brazil Intern. Conference on Fatigue (SAE Brasil - Seção São Paulo)*, June 22-23th, 2004, São Paulo, Brazil.
- Saouridis, C. & Mazars, J., "A Multiscale Approach to Distributed Damage and its Usefulness for Capturing Structural Size Effect", *In Cracking and Damage (Edited by J. Mazars and Z. P. Bazant)*, pp. 391-403. Elsevier, Amsterdam, 1988.
- Simo, J.C., and Miehe, C., "Associative Coupled Thermoplasticity at Finite Strains: Formulation, Numerical Analysis and Implementation", *Computer Methods in Applied Mechanics and Engineering*, Vol. 98, pp. 41-104 (1992).

- Vree, J.H.P. de, Brekelmans, W.A.M, and Gils, M.A.J. van, "Comparison of Nonlocal Approaches in Continuum Damage Mechanics", *Computer and Structures*, Vol. 55, N°4, pp. 581-588 (1995).
- Yanenko, N.N., "The Method of Fractional Steps", *Springer-Verlag*, New York, 1980.